Taylor & Francis
Taylor & Francis Group

Philosophical Magazine

ISSN: 1478-6435 (Print) 1478-6443 (Online) Journal homepage: http://www.tandfonline.com/loi/tphm20

# Structural and electronic properties of $InN_xP_{1-x}$ alloy in full range ($0 \leq x \leq 1$)

**Metin Aslan, A. H. Reshak, Battal G. Yalcin, Sadik Bagci & Mehmet Ustundag**

**To cite this article:** Metin Aslan, A. H. Reshak, Battal G. Yalcin, Sadik Bagci & Mehmet Ustundag (2016): Structural and electronic properties of $InN_xP_{1-x}$ alloy in full range ($0 \leq x \leq 1$), Philosophical Magazine, DOI: 10.1080/14786435.2016.1149248

**To link to this article:** http://dx.doi.org/10.1080/14786435.2016.1149248

Published online: 03 Mar 2016.

Submit your article to this journal

View related articles

View Crossmark data

Full Terms & Conditions of access and use can be found at
http://www.tandfonline.com/action/journalInformation?journalCode=tphm20

**Download by:** [Zapadoceska Univerzita], [A Reshak] **Date:** 03 March 2016, At: 07:57

PHILOSOPHICAL MAGAZINE, 2016
http://dx.doi.org/10.1080/14786435.2016.1149248

Taylor & Francis
Taylor & Francis Group

# Structural and electronic properties of $InN_xP_{1-x}$ alloy in full range ($0 \le x \le 1$)

Metin Aslan[a], A. H. Reshak[b,c], Battal G. Yalcin[a], Sadik Bagci[a] and Mehmet Ustundag[a]

[a]Science and Art Faculty, Physics Department, Sakarya University, Sakarya, Turkey; [b]New Technologies – Research Centre, University of West Bohemia, Pilsen, Czech Republic; [c]School of Material Engineering, Center of Excellence Geopolymer and Green Technology, University Malaysia Perlis, Kangar, Malaysia

**ABSTRACT**

We have performed first-principles method to investigate structural and electronic properties of $InN_xP_{1-x}$ ternary semiconductor alloy in full range ($0 \le x \le 1$) using density functional theory. We have used modified Becke–Johnson potential to obtain accurate band gap results. From the electronic band structure calculation we have found that $InN_xP_{1-x}$ become metal between 47 and 80% of nitrogen concentration. Additional to our band gap calculations, we have also used the band anticrossing model. The band anticrossing model supplies a simple, analytical expression to calculate the physical properties, such as the electronic and optical properties, of III-$N_xV_{1-x}$ alloys. The knowledge of the electron density of states is required to understand and clarify some properties of materials such as the band structures, bonding character and dielectric function. In order to have a deeper understanding of these properties of the studied materials, the total and partial density of states has been calculated. Finally, we have calculated the total bowing parameter b of studied alloys, together with three contributions $b_{VD}$, $b_{CE}$, and $b_{SR}$ due to volume deformation, different atomic electron negativities and structural relaxation, respectively.

**ARTICLE HISTORY**
Received 12 October 2015
Accepted 27 January 2016

**KEYWORDS**
Semiconductor alloys; density functional theory; structural properties; electronic properties; bowing parameter

Downloaded by [Zapadoceska Univerzita], [A Reshak] at 07:57 03 March 2016

## 1. Introduction

Among group III–V compound semiconductors, *InN* [1] and *InP* [2] are extremely important materials over the past decade. *InN* is a widely used semiconductor material because its low temperature dependence, high carrier mobility and low electron effective mass, which can be used in photovoltaic devices, high frequency transmitters and high frequency detectors [3]. As a semiconductor with a direct band gap, *InP* possesses many superior properties such as high thermal conductivity, high saturation field electron drift rate, high carrier mobility and high absorption coefficient for photons whose energy is larger than the band gap of *InP*, which are promising for extensive applications in biological sensors, anti-radiation solar cells, liquid crystal displays, fibre communications, laser chips

**CONTACT** Metin Aslan maslan@sakarya.edu.tr

© 2016 Taylor & Francis

and communication satellites [4,5]. Moreover, because of high electron mobility, band gap around 1.5 eV and good heat conducting properties of *InP* find its potential application in microwave and optoelectronic devices. Recently, doped phosphide semiconductor alloys have drawn much attention due to their special characters. A small amount of nitrogen incorporation into *InP* will drastically decrease the band-gap energy of this material, making it suitable specially for long wave length device application. The effect of small amount of *N* to host *InP* has been studied experimentally by some groups [6,7]. This reduction of the band gap in III-NV alloys was explained by an interaction between the localized nitrogen resonant levels and the extended band states of the host semiconductor matrix materials. Not only a small amount of nitrogen, the investigation of ternary $InN_xP_{1-x}$ alloys in full range ($0 \leq x \leq 1$) is also very important for many application like terahertz imaging systems and thermoelectric power generators because of the ability to reach very narrow band gaps. With full range investigation, it could be obtained at which amount of nitrogen could *InNP* become a metal and become a semiconductor again. Another important point is, to be grown the material lattice matched on a particular substrates like silicon and GaAs. This can be seen with investigating the alloy in full range. Our study could provide new information on the occurrence of new applications.

## 2. Computational details

All-electron-full-potential (linearized) augmented plane wave plus local orbitals (FP-(L) APW + lo) method as implemented in WIEN2k [8] is used to perform a comprehensive theoretical calculation. This is a very precise and efficient approach to solve the Kohn–Sham equation within a framework of density functional theory (DFT). Within a framework of this approach, the potential and corresponding charge density is expanded into lattice harmonics inside each atomic sphere and as a Fourier series in the interstitial region. It is well known that in the self-consistent band structure calculation within DFT, both the local density approximation (LDA) [9] and the generalized gradient approximation (GGA) [10] approaches usually underestimate the energy gap [11,12]. This is mainly due to the fact that they are based on simple model assumptions, which are not sufficiently flexible to accurately reproduce the exchange correlation energy and its charge space derivative. Therefore, we have used the recently modified Becke–Johnson potential (mBJ) [13] to obtain accurate band gap while for structural properties the GGA of Wu–Cohen (WC) [14] was applied.

The semi-local Becke–Johnson (BJ) exchange-correlation potential and its modified form proposed by Tran and Blaha have attracted a lot of interest recently because of the surprisingly accurate band gaps they can deliver for many semiconductors and insulators (e.g., sp semiconductors, noble-gas solids and transition-metal oxides). Since standard semi-local GGA underestimates band gaps [15], the exchange and correlation effects of self-consistent band structures are also treated by using the modified mBJ potential [16]. This method is a modified version of the mBJ potential used to improve band gaps obtained by the conventional DFT-based methods. The mBJ potential can be written as:

$$\upsilon_{x,\sigma}^{mBJ}(\vec{r}) = c\upsilon_{x,\sigma}^{BR}(\vec{r}) + (3c-2)\frac{1}{\pi}\sqrt{\frac{5}{6}}\sqrt{\frac{\tau_\sigma(\vec{r})}{\rho_\sigma(\vec{r})}} \tag{1}$$

Downloaded by [Zapadoceska Univerzita], [A Reshak] at 07:57 03 March 2016

where $\rho_\sigma$ is the electron density, $\tau_\sigma$ is the kinetic-energy and $v_{x,\sigma}^{BR}$ is the Becke–Roussel potential [17]. The $c$ parameter is a system-dependent parameter, with $c = 1$ corresponding to the original Becke–Johnson potential. For bulk crystalline materials, Tran and Blaha proposed to determine $c$ by the following empirical relation:

$$c = \alpha + \beta\left(\frac{1}{V_{cell}}\int_{cell}\frac{|\nabla\rho_\sigma(r')|}{\rho_\sigma(r')}d^3r'\right)^{\frac{1}{2}} \tag{2}$$

where $V_{cell}$ means the unit cell volume, $\alpha = -0.012$ and $\beta = 1.023$ bohr$^{1/2}$ are parameters fitted according to experimental values [13].

It is important to point out that mBJ is a potential-only functional, i.e., there is no corresponding mBJ exchange-correlation energy. This fact, therefore leads to the impossibility of using mBJ to compute Hellmann–Feynman forces and to compare total energies [18]. Using this modified Becke–Johnson potential, the band gaps of many insulating systems can be described accurately with an effort that is in general comparable to that of LDA or GGA [11–13]. For electronic structure calculations, the mBJ potential is used to yield quite accurate gaps for numerous semiconductors [11,13,19], wide band-gap insulators, sp semiconductors, 3d transition-metal oxides [13,20] and doped semiconductors systems [21].

A fully relativistic calculation and scalar relativistic approximation for core and valance states, respectively, without spin–orbit interaction were used. In the interstitial region, the plane wave cut-off value of $R_{MT}K_{\max} = 6$ was used. Inside the atomic spheres maximum value of angular momentum $l_{\max} = 10$ , was taken for the wave function expansion. For Fourier expansion of potential in the interstitial region, the charge density was expanded up to $G_{\max} = 12$ Ry$^{1/2}$. The separation energy among the valence and core states was chosen to be −6.0 Ry. The standard special $k$-points technique of Monkhorst and Pack (MP) [22] was used for accurate Brillouin zone (BZ) integrations. A $\boldsymbol{k}$-mesh of 2 × 2 × 2 and 36 × 36 × 36 is taken for the considered ternary alloys and binary compounds, respectively, in the irreducible wedge of the BZ. Self-consistent calculations are considered to be converged when the energy difference between succeeding iterations is less than $10^{-6}$ Ry. For a wellforce, charge convergence of crystal system is stable within less than 0.0001 e. In the considered alloy structure, free coordinates of atoms were relaxed using the quantum mechanical forces, so residual forces on the ions were <1 mRy/bohr. The $\boldsymbol{k}$ meshes and basis sets were chosen to be good enough such that the presented results were well converged.

## 3. Results and discussion

### 3.1 Structural properties

In this section, we present the structural properties of ternary alloys $InN_xP_{1-x}$ for composition of $0 \le x \le 1$. The binary compounds $InP$ and $InN$ are described by 1 × 1 × 1 conventional face centred cubic cell while the ternary alloys $InN_xP_{1-x}$ are modelled with 64 atom multiplicity of primitive simple cubic 2 × 2 × 2 supercell with 3.125% intervals of $x$. The calculated total energies were fitted to the Murnaghan's equation of state [23] in order to obtain the ground state properties such as equilibrium lattice constant ($a_0$) and bulk modulus ($B_0$).

Downloaded by [Zapadoceska Univerzita], [A Reshak] at 07:57 03 March 2016

Downloaded by [Zapadoceska Univerzita], [A Reshak] at 07:57 03 March 2016

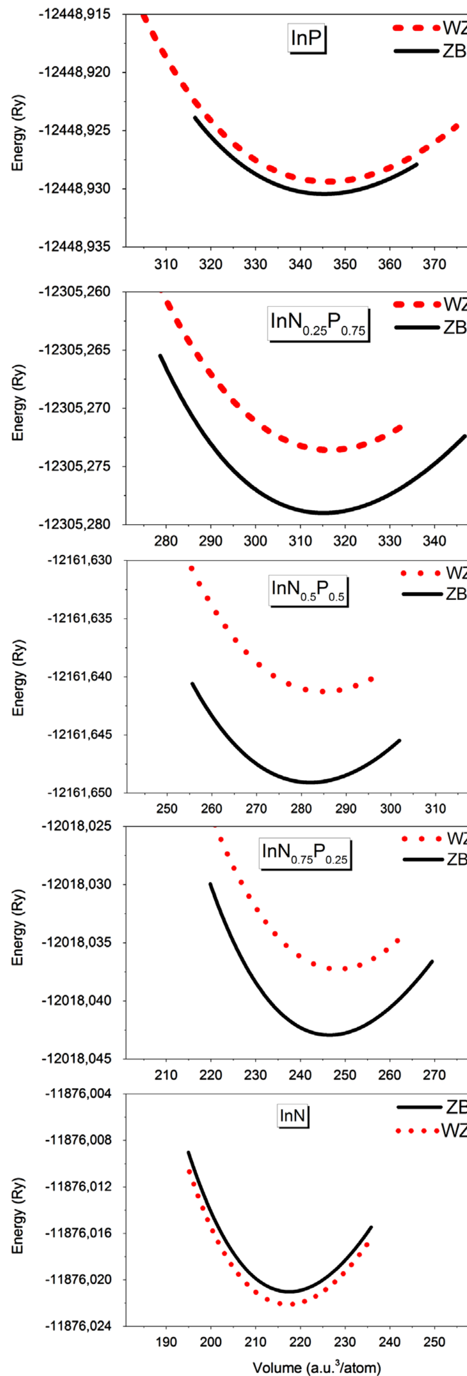


**Figure 1.** (colour online) Total energies as a function of volume for the $InN_{1-x}P_x$ alloys for ZB and WZ phases.

We first perform the total energies for the zincblende (ZB) and wurtzite (WZ) structures as a function of volume in order to determine the optimized structural phase stability for the studied materials. Figure 1 shows the behaviour of the total energy versus volume

**Table 1.** The calculated structural properties of the studied binary compounds, InN and InP.

| Binary compounds | $a_0$ (A) | $B_0$ (GPa) |
|---|---|---|
| *InN* | 5.897 | 67.5 |
| | 5.867 [24], 5.869 [25], 5.869 [26] (exp) | 71 [34], 67 [35] (exp) |
| | 5.729 (PW-PP) [27] | |
| | 6.014 (FP-LMTO) [28] | 60 [28] |
| *InP* | 5.001 | 140 |
| | .986 [29], 4.98 [30], 5.01 ± 0.1 (10 K) [31] (exp) | 136 [36] (exp) |
| | 4 4.957 (LDA) [32] | 183.3 [32] |
| | 5.11(GGA) [33] | 118 [33] |

Downloaded by [Zapadoceska Univerzita], [A Reshak] at 07:57 03 March 2016

curves for ZB and WZ structures of studied compounds and ternary alloys. As can be seen from Figure 1, the ZB phase is found to be more stable than the other possible phase for *InP* and $InN_xP_{1-x}$ alloys. On the other hand, the WZ phase found to be the ground state of *InN*. There is a very low energy difference (~0.001 Ry) between ZB and WZ phases for *InN*. Therefore, we have considered all studied materials in ZB phase in order to compare them with each other.

The obtained structural properties of binary compounds are summarized in Table 1 together with available theoretical [27,28,32,33] and experimental [24–26,29–31,34–36] results. The calculated lattice parameters for *InP* and *InN* are found to be 5.897 and 5.001 Å, respectively. The results show that the equilibrium lattice parameters of considered binary compounds are in excellent agreement with the experimental data [24–26,29–31] indicating the reliability of present calculation. Our predicated theoretical results overestimated the experimental lattice parameters by less than 0.5%, which is a typical consequence of the GGA calculations. The calculated bulk modulus of the binary compounds is presented in Table 1 which indicates good agreement with the experimental [34–36] and theoretical [28,32,33] results. Our calculated value for bulk modulus of *InP* (67.5 GPa) is 0.75% larger than the experimental value (67 GPa) [35]. The calculated bulk modulus of *InN* is found to be 140 GPa in good agreement with the experimental value (136 GPa) [36].

The obtained structural properties of the ternary alloys are summarized in Table 2. The compressibility of the studied alloy increased when *N* concentration increased as expected. The treatment of lattice parameters of ternary alloys can be defined as a linear combination of the lattice constants of the two forming binary compounds. Therefore, it is assumed that the atoms are located at the ideal lattice sites and the lattice constant varies linearly with composition $x$ according to the so-called Vegard's law [37]

$$a(AB_{1-x}C_x) = (1-x)a_{AB} + xa_{AC} \tag{3}$$

where $a_{AB}$ and $a_{AC}$ are the equilibrium lattice constants of binary *AB* and *AC* compounds, respectively, and $a(AB_{1-x}C_x)$ is the alloy lattice constant.

The results of the equilibrium lattice constants for ternary alloys $InN_xP_{1-x}$ as a function of $x$ are presented in Figure 2. It shows good agreement with those estimated by Vegard's law. To the best of our knowledge no comprehensive work neither experimental data nor first -principles calculations on the structural properties of ternary alloys $InN_xP_{1-x}$ at the range of $0 \le x \le 1$ have appeared in the literature to make a meaningful comparison. Hence, our results can serve as a reference for future investigations. In order to understand the interfaces and proximity effects of substrates on our investigated alloys, we presented the

**Table 2.** The calculated structural properties of the studied ternary alloys, $InN_xP_{1-x}$.

| Ternary alloys $InN_xP_{1-x}$ ($x$) | $a_0$ (A) | $B_0$ (GPa) |
|---|---|---|
| 0.03125 | 5.852 | 68.880 |
| 0.0625 | 5.820 | 70.200 |
| 0.09375 | 5.795 | 72.017 |
| 0.125 | 5.771 | 73.881 |
| 0.15625 | 5.742 | 75.772 |
| 0.1875 | 5.712 | 77.366 |
| 0.21875 | 5.680 | 78.966 |
| 0.28125 | 5.628 | 80.026 |
| 0.34375 | 5.569 | 81.639 |
| 0.40625 | 5.515 | 86.226 |
| 0.46875 | 5.464 | 95.746 |
| 0.53125 | 5.405 | 98.532 |
| 0.59375 | 5.346 | 99.542 |
| 0.65625 | 5.293 | 102.421 |
| 0.71875 | 5.239 | 105.446 |
| 0.78125 | 5.181 | 114.044 |
| 0.8125 | 5.157 | 116.564 |
| 0.84375 | 5.124 | 118.151 |
| 0.875 | 5.096 | 120.343 |
| 0.90625 | 5.069 | 131.623 |
| 0.9375 | 5.037 | 135.254 |
| 0.96875 | 5.014 | 138.882 |

Downloaded by [Zapadoceska Univerzita], [A Reshak] at 07:57 03 March 2016

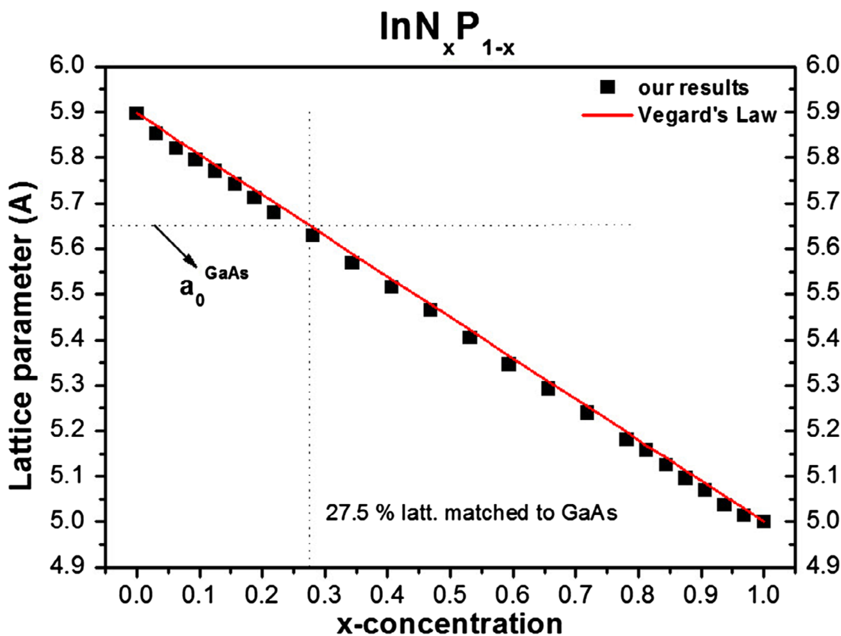


**Figure 2.** (colour online) Composition dependence of the calculated lattice parameter of ternary alloys $InN_xP_{1-x}$ with Vegard's prediction.

properties of $InN_xP_{1-x}$ alloys lattice matched to GaAs semiconductor substrate. From Figure 2, the crossover of the dotted lines indicates that the ternary alloys $InN_xP_{1-x}$ is expected to be lattice matched to the GaAs substrate for a composition equal to ~27.5%. The lattice parameter of GaAs is taken to be an experimental value of 5.653 Å [38].

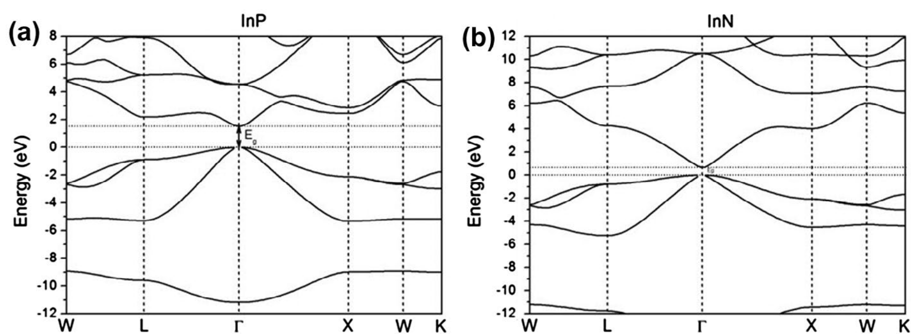


**Figure 3.** Electronic band structure of (a) *InP* and (b) *InN* within the mBj calculation.

Downloaded by [Zapadoceska Univerzita], [A Reshak] at 07:57 03 March 2016

### *3.2. Electronic properties*

It is well known that in standard density functional calculations both GGA and LDA underestimate the band gap of semiconductors since quasiparticle excitations are not consider in DFT. To overcome this drawback, we have used the mBJ approach, which brings the calculated gap close to the measured one. The mBJ gives a similar precision as obtainable with computationally more expensive hybrid functional and GW methods [19].

Figure 3 shows the band structure of both studied binary compounds *InP* and *InN*, along the high-symmetry lines across the first irreducible Brillouin zone calculated within mBJ approximation. The valance band maximum (VBM) and the conduction band minimum (CBM) occur at the Γ point indicating that these materials have a direct band gap. These results agree well with the previous experimental and theoretical findings. The calculated fundamental band gaps for the studied binary compounds are summarized in Table 3 together with previous theoretical works [39,40] as well as experimental data [41,42]. The calculated band gap of *InP* and *InN* is 1.53 and 0.65 eV using mBJ, in comparison to experimental band gap 1.42 eV (*InP*) [41] and 0.61 eV (*InN*) [42], which are much better than previous calculations using GGA and LDA [39,40]. Therefore, mBJ succeeds to bring the calculated energy gap close to the measured one. In Table 3, we have also tabulated the fundamental band gaps for the studied ternary alloys. Unfortunately, there is neither theoretical nor experimental data for comparison. There have been numerous attempts to explain the band structure properties of the group III-V*N* alloys. The unusual properties of the III-$N_xV_{1-x}$ alloys can be well explained by the recently proposed, band anticrossing (BAC) model [43]. The BAC model supplies a simple, analytical expression to calculate the physical properties, such as the electronic and optical properties, of III-$N_x$ $V_{1-x}$ alloys. According to the BAC model, a repulsive interaction between the localized nitrogen states, which are located above the conduction band edge, and the extended states of the host semiconductor matrix splits the conduction band of the matrix semiconductor into two sub-bands. The downward shift of the lower sub-band is responsible for the reduction of the fundamental band gap and optical transitions from valance band to the upper sub-band account for the high-energy edge [44].

According to the BAC model, if the effect on the valence bands is completely neglected, the dispersion relations for the upper and lower conduction sub-bands, $E_+$ and $E_-$ are given by [43]

**Table 3.** Direct (Γ-Γ) band gaps of InN, InP and their ternary alloys at equilibrium volume.

| Materials $InN_xP_{1-x}$ | $E_g$ (eV) (Γ–Γ) | References |
|---|---|---|
| *InP* | 1.53 | This work (mBJ) |
| | 1.42 | Exp (6 K) [41] |
| | 0.62 | Theory (LDA) [40] |
| | 0.85 | Theory (GGA) [40] |
| Ternary alloys | | |
| 0.03125 | 1.19816 | This work (mBJ) |
| 0.0625 | 1.19608 | This work (mBJ) |
| 0.09375 | 0.93455 | This work (mBJ) |
| 0.125 | 0.97821 | This work (mBJ) |
| 0.15625 | 0.68798 | This work (mBJ) |
| 0.1875 | 0.69513 | This work (mBJ) |
| 0.21875 | 0.47563 | This work (mBJ) |
| 0.28125 | 0.35477 | This work (mBJ) |
| 0.34375 | 0.207 | This work (mBJ) |
| 0.40625 | 0.08663 | This work (mBJ) |
| 0.46875 | $9 * 10^{-5}$ | This work (mBJ) |
| 0.53125 | Metal | This work (mBJ) |
| 0.59375 | Metal | This work (mBJ) |
| 0.65625 | Metal | This work (mBJ) |
| 0.71875 | Metal | This work (mBJ) |
| 0.78125 | Metal | This work (mBJ) |
| 0.8125 | 0.05763 | This work (mBJ) |
| 0.84375 | 0.17422 | This work (mBJ) |
| 0.875 | 0.32949 | This work (mBJ) |
| 0.90625 | 0.4017 | This work (mBJ) |
| 0.9375 | 0.57933 | This work (mBJ) |
| 0.96875 | 0.60955 | This work (mBJ) |
| *InN* | 0.65 | This work (mBJ) |
| | 0.61 | Exp (10 K) [42] |
| | 0.54 | Theory (LDA) [39] |
| | 0.264 | Theory (GGA) [39] |

$$E_{\pm}(k) = \frac{1}{2\left\{E_N + E_M(k) \pm \sqrt{[E_N - E_M(k)]^2 + 4C_{NM}^2 x}\right\}} \tag{4}$$

where $E_N$ is the energy of the $N$ level, $E_M(k)$ is the standard parabolic dispersion relation for the host semiconductor matrix, and $C_{NM}$ is the matrix element describing the coupling between $N$ states and the extended states.

Figure 4 shows the fundamental band gap of $InP_{1-x}N_x$ alloys as a function of $N$ concentration together with the dependence calculated from the BAC model. The corresponding calculated data are shown by solid (closed) star while dashed line shows polynomial fitting in Figure 4. The solid line in Figure 4 is the $E_-$ energy calculated by the BAC model, using the known band structure parameters of the $InP$ matrix, $E_M = 1.53$ eV. The energy of the highly localized nitrogen level $E_N = 2$ eV relative to the valance band edge in $InP$ was estimated from the valance band offset ΔeV(GaAs/$InP$) = 0.35 eV [2,44]. We found that, for zero temperature, the obtained data in Figure 4 are best described with a coupling matrix element $C_{NM} = 2.7$ eV. As can be seen from Figure 4, our calculated data are in good agreement with the theoretical calculation from BAC model.

The knowledge of the electron density of states (DOS) is required to understand and clarify some properties of materials such as the band structures, bonding character and

Downloaded by [Zapadoceska Univerzita], [A Reshak] at 07:57 03 March 2016

Downloaded by [Zapadoceska Univerzita], [A Reshak] at 07:57 03 March 2016

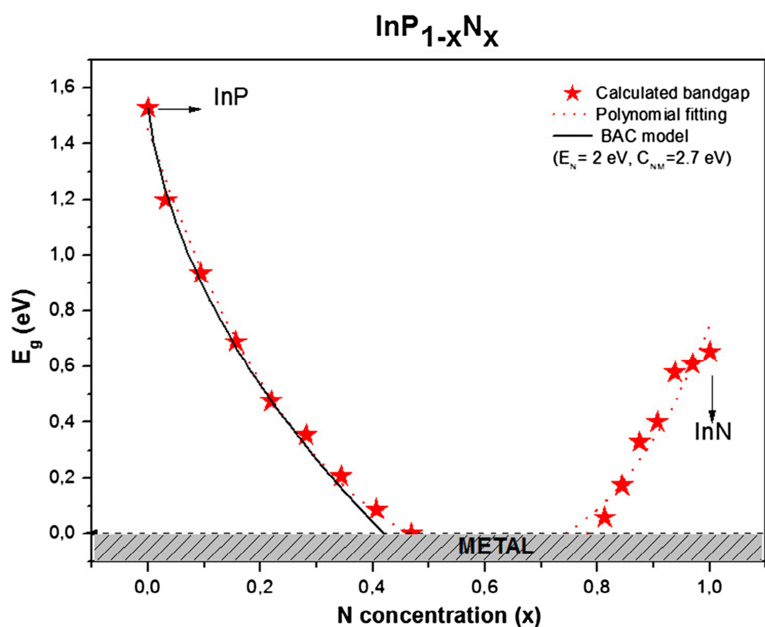


**Figure 4.** (colour online) Energy gap of $InN_xP_{1-x}$ as a function of $N$ concentration. The solid curve is the fitting of the BAC model. The dashed curve shows polynomial fitting.

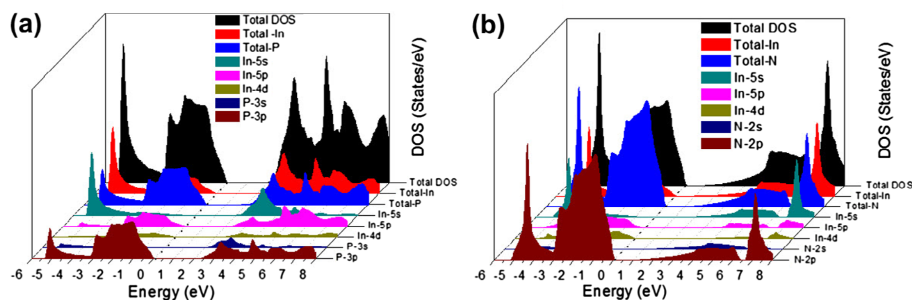


**Figure 5.** (colour online) The calculated total and partial density of states for (a) *InP* and (b) *InN* compound. The Fermi level is set to 0 eV.

dielectric function. In order to have a deeper understanding of these properties of the studied materials, the total and partial density of states has been calculated.

The total density of states and partial density of states for studied binary compounds, *InP* and *InN*, are shown in Figure 5(a) and (b), respectively, as obtained by means of the mBJ scheme. It is clearly shown from Figure 5(a), the states below $E_F$ mainly originates from the hybridization of *In* 5p and *P* 3p states. While the lower part of conduction band close to $E_F$ shows a strong hybridization of *In* 5s and *P* 3p states. The density of states for *InN* is shown in Figure 5(b). The calculated DOS is very similar to that for *InP*. The states between 0 and −5 eV below $E_F$ are mainly occupied by *In* 5s and *N* 2p states. The lower part of the conduction band close to $E_F$ is heavily dominated by *N* 2p electrons.

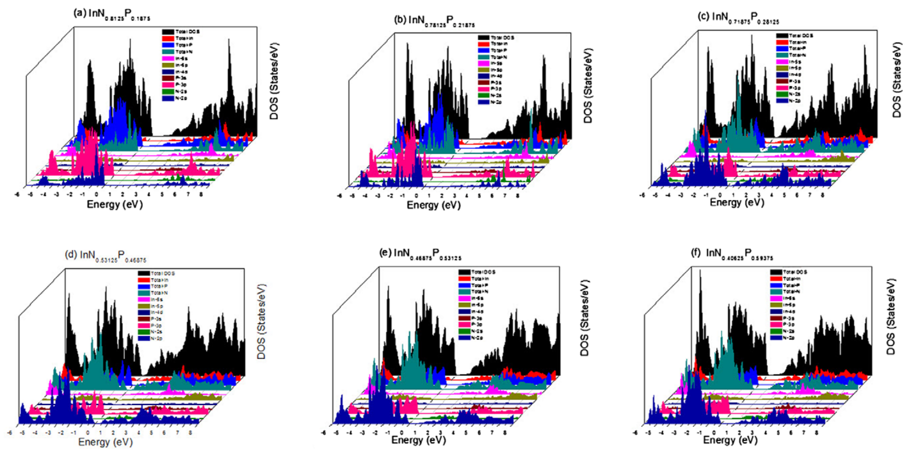


**Figure 6.** (colour online) The calculated total and partial density of states for (a) $InN_{0.8125}P_{0.1875}$, (b) $InN_{0.78125}P_{0.21875}$, (c) $InN_{0.71875}P_{0.28125}$, (d) $InN_{0.53125}P_{0.46875}$, (e) $InN_{0.46875}P_{0.53125}$ and (f) $InN_{0.40625}P_{0.59375}$ alloys. The Fermi level is set to 0 eV.

We have also calculated the total and partial density of states for some selected ternary alloys as shown in Figure 6(a–f). In these figures, the $E_F$ is arbitrarily shifted to the origin. The studied ternary alloys, except of $InN_{0.71875}P_{0.28125}$ and $InN_{0.53125}P_{0.46875}$ alloys, show a distinct energy gap between the valance and the conduction energy bands, the alloy system retaining its semiconductor character. On the other side, the occupied conduction electron states are in $InN_{0.71875}P_{0.28125}$ and $InN_{0.53125}P_{0.46875}$ alloys heavily dominated by $N$ 2p electrons. It can be seen that there are some bands crossing the $E_F$, which indicates metallic behaviour of $InN_{0.71875}P_{0.28125}$ and $InN_{0.53125}P_{0.46875}$ ternary alloys (see Table 3).

In order to better analyse the physical origins of the band gap bowing parameter in $InN_xP_{1-x}$ alloys, we follow the approach of Bernard and Zunger [45]. In this approach, the total bowing parameter '$b$' is assumed to be independent of composition $x$ and is decomposed into three components. The overall bowing coefficient at a given average composition $x$ measures the change in band gap according to the formal reaction:

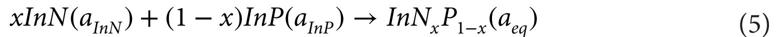

$$xInN(a_{InN}) + (1-x)InP(a_{InP}) \rightarrow InN_xP_{1-x}(a_{eq}) \quad (5)$$

where $a_{InN}$ and $a_{InP}$ are the equilibrium lattice constants of the studied binary compounds $InN$ and $InP$, respectively, $a_{eq}$ is the equilibrium lattice constants of the alloy with the average composition of $x$. Equation (5) is decomposed into three steps:

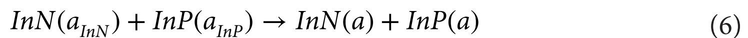

$$InN(a_{InN}) + InP(a_{InP}) \rightarrow InN(a) + InP(a) \quad (6)$$

$$xInN(a) + (1-x)InP(a) \rightarrow InN_xP_{1-x}(a) \quad (7)$$

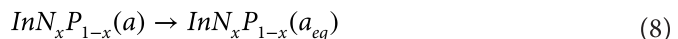

$$InN_xP_{1-x}(a) \rightarrow InN_xP_{1-x}(a_{eq}) \quad (8)$$

The first step measures the volume deformation (VD) effect on the bowing. The corresponding contribution $b_{VD}$ to the total bowing parameter represents the relative response of the

Downloaded by [Zapadoceska Univerzita], [A Reshak] at 07:57 03 March 2016

**Table 4.** Decomposition of optical bowing into contributions due to volume deformation (VD), charge exchange (CE) and structural relaxation (SR), compared with that obtained by a quadratic interpolation (all values in eV).

| $InN_xP_{1-x}$ (x) | $b_{VD}$ | $b_{CE}$ | $b_{SR}$ | $b$ | Quadratic equation (Equation 7) |
|---|---|---|---|---|---|
| 0.03125 | 12.84649 | −1.54963 | −1.22318 | 10.07368 | 10.07 |
| 0.09375 | 8.29582 | −1.88576 | −0.35051 | 6.059549 | 6.06 |
| 0.875 | 2.260663 | 2.082377 | −0.24695 | 4.096091 | 4.1 |
| 0.9375 | 2.517323 | 0.626528 | −0.67908 | 2.464768 | 2.46 |
| 0.96875 | 2.926803 | 0.944083 | −0.98634 | 2.884542 | 2.88 |

band structure of the binary compounds *InN* and *InP* to hydrostatic pressure, which here arises from the change of their individual equilibrium lattice constants to the alloy value $a = a(x)$. The second contribution, the charge exchange (CE) contribution $b_{CE}$, reflects a charge transfer effect which is due to the different (averaged) bonding behaviour at the lattice constant $a$. The final step, the structural relaxation (SR), measures changes in passing from the unrelaxed to the relaxed alloy by $b_{SR}$. Consequently, the total bowing parameters defined as

$$b = b_{VD} + b_{CE} + b_{SR} \tag{9}$$

The general representation of the composition-dependent band gap of the alloys in terms of the gaps of the binary compounds, $E_{InN}(a_{InN})$ and $E_{InP}(a_{InP})$, and the total bowing parameter $b$ is;

$$Eg(x) = xE_{InN}(a_{InN}) + (1-x)E_{InP}(a_{InP}) - bx(1-x) \tag{10}$$

This allows a division of the total bowing b into three contributions according to

$$b_{VD} = \frac{E_{InN}(a_{InN}) - E_{InN}(a)}{1-x} + \frac{E_{InP}(a_{InP}) - E_{InP}(a)}{x} \tag{11}$$

$$b_{CE} = \frac{E_{InN}(a)}{1-x} + \frac{E_{InP}(a)}{x} - \frac{E_{InPN}(a)}{x(1-x)} \tag{12}$$

$$b_{SR} = \frac{E_{InPN}(a) - E_{InPN}(a_{eq})}{x(1-x)} \tag{13}$$

where $E$ is the energy band gap calculated for the indicated compound with the indicated atomic positions and lattice constant $a_{InN}$, $a_{InP}$ and $a_{eq}$ are the equilibrium lattice constants of *InN*, *InP* and $InN_xP_{1-x}$ alloys, respectively. The lattice constant (a) is calculated by linear composition dependence rule for the alloys. All these energy gaps occurring in expressions (8)–(10) have been calculated for the indicated atomic structures and lattice constants.

Using Equations (11)–(13), the total bowing parameter b, together with three contributions $b_{VD}$, $b_{CE}$, and $b_{SR}$ due to volume deformation, different atomic electron negativities, and structural relaxation, respectively, calculated at a wide range of composition $0.03125 \le x \le 0.96875$ for $InN_xP_{1-x}$ alloy are listed in Table 4, together with the bowing

Downloaded by [Zapadoceska Univerzita], [A Reshak] at 07:57 03 March 2016

Downloaded by [Zapadoceska Univerzita], [A Reshak] at 07:57 03 March 2016

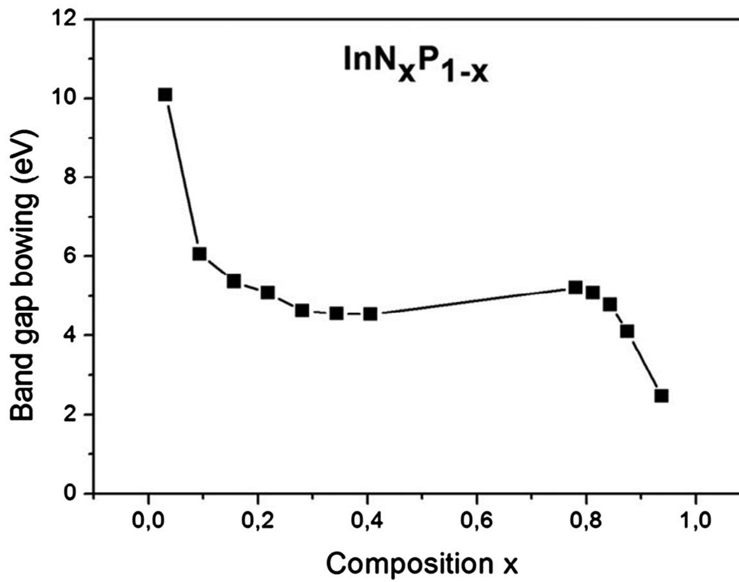


**Figure 7.** The calculated band gap bowing parameter as function of nitrogen composition.

obtained using a quadratic variation of the band gap versus composition $x$. The calculated quadratic parameters of the gap bowing are in good agreement with the values found from the approach of Bernard and Zunger [45].We have presented the variation of the band gap bowing versus concentration as shown in Figure 7. It is clear that the main contribution to total gap bowing of $InN_xP_{1-x}$ alloy raises from the volume deformation effect represented by $b_{VD}$. This is related to the strong mismatch of the lattice parameters of *InN* and *InP* compounds. Because of the ordered structure, the contribution of the structural relaxation $b_{SR}$ to the bowing parameter is small. The charge transfer contribution $b_{CE}$ has weak contribution at the total gap bowing parameter; this is related to electronegativity mismatch between the constituting atoms: *In* (1.78), *N* (3.04) and *P* (2.19).

## 4. Conclusions

In this study, we have calculated structural and electronic properties of $InN_xP_{1-x}$ alloy in full range of nitrogen. All-electron-full-potential (linearized) augmented plane wave plus local orbitals (FP-(L)APW + lo) method as implemented in WIEN2k is used to perform a comprehensive theoretical calculation.

We have firstly presented phase stability calculations for *InN*, *InP* and $InN_xP_{1-x}$ ($x = 0.25$, 0.50, and 0.75) alloys. Our results for total energy calculations indicate that the zincblende structure is the most stable phase for all the selected materials. The calculated lattice parameters for considered binary compounds are in excellent agreement with previous experimental results. We have also presented equilibrium lattice constants for ternary alloys $InN_xP_{1-x}$ as a function of $x$ and the results are in accordance with Vegard's law. These results also indicated that $InN_xP_{1-x}$ is expected to be lattice matched to the GaAs substrate for $x$ value of ~27.5%. We have used the recently modified Becke–Johnson potential (mBJ) to obtain accurate band gap for *InN*, *InP* and $InN_xP_{1-x}$ alloys. The calculated band gap values of *InP*

and $InN$ are found to be 1.53 and 0.65 eV, respectively, and these results are consistent with previous experimental band gap values. We have also calculated the band gap values for $InN_xP_{1-x}$ alloys with 3.125% intervals of $x$. The band gap variation with $N$ concentration indicates that $InN_xP_{1-x}$ becomes metal between 47 and 80% of nitrogen. This variation also shows that our calculated results are in good agreement with the theoretical calculation from BAC model. The total and partial density of states have been calculated for the binary compounds and some selected ternary alloys. The calculated DOS shape of $InN$ is similar to that for $InP$. The selected ternary alloys, except of $InN_{0.71875}P_{0.28125}$ and $InN_{0.53125}P_{0.46875}$ alloys, show semiconductor character with an energy band gap. We have found that $InN_{0.71875}P_{0.28125}$ and $InN_{0.53125}P_{0.46875}$ alloys have a metallic behaviour because some bands cross the Fermi level. The unoccupied conduction electron states for these alloys are heavily dominated by $N$ 2p electrons.

Finally, we have presented the total bowing parameter b, together with its three components $b_{VD}$, $b_{CE}$, and $b_{SR}$ at a wide range of composition $0.03125 \leq x \leq 0.96875$ for $InN_xP_{1-x}$ alloys. We have found that the main contribution to the total gap bowing of $InN_xP_{1-x}$ alloy raises from the volume deformation effect represent by $b_{VD}$ and this is related to the strong mismatch of the lattice parameters of $InN$ and $InP$ compounds.

## Acknowledgements

The author A.H. Reshak would like to acknowledge the CENTEM project, reg. No. CZ.1.05/2.1.00/03.0088, cofunded by the ERDF as part of the Ministry of Education, Youth and Sports OP RDI programmme and, in the follow up sustainability stage, supported through CENTEM PLUS (LO1402) by financial means from the Ministry of Education, Youth and Sports under the National Sustainability Programme I. Computational resources were provided by MetaCentrum (LM2010005) and CERIT-SC (CZ.1.05/3.2.00/08.0144) infrastructures.

## Disclosure statement

No potential conflict of interest was reported by the authors.

## References

[1] F. Werner, F. Limbach, M. Carsten, C. Denker, J. Malindretosand and A. Rizzi, *Electrical Conductivity of InN Nanowires and the Influence of the Native Indium Oxide Formed at Their Surface*, Nano Lett. 9 (2009) p.1567–1571.

[2] C.J. Novotny, E.T. Yuand and P.K.L. Yu, *InP nanowire/polymer hybrid photodiode*, Nano Lett. 8 (2008) p.775–779.

[3] M.C. Johnson, C.J. Lee, E.D. Bourret-Courchesne, S.L. Konsek, S. Aloni, W.Q. Han and A. Zettl, *Growth and morphology of 0.80eV 0.80eV photoemitting indium nitride nanowires*, Appl. Phys. Lett. 85 (2004) p.5670–5672.

[4] T.J. Kempa, B. Tian, D.R. Kim, J. Hu, X. Zhengand and C.M. Lieber, *Single and tandem axial p-i-n nanowire photovoltaic devices*, Nano Lett. 8 (2008) p.3456–3460.

[5] C. Battaglia, J. Xu, M. Zheng, X. Yin, M. Hettick, K. Chen, N. Haegeland and A. Javey, *Enhanced near-bandgap response in InP nanopillar solar cells*, Adv. Energy Mater. 1400061 (2014) p.1–5.

[6] W.G. Bi and C.W. Tu, *N incorporation in InP and band gap bowing of InN x P1−x*, J. Appl. Phys. 80 (1996) p.1934–1936.

Downloaded by [Zapadoceska Univerzita], [A Reshak] at 07:57 03 March 2016

[7] K.M. Yu, W. Walukiewicz, J. Wu, J. Beeman, J.W. Ager III, E.E. Haller, W. Shan, H.P. Xin and C.M. Tu, *Synthesis of InN x P 1−x thin films by N ion implantation*, Appl. Phys. Lett. 78 (2001) p.1077–1079.

[8] P. Blaha, K. Schwarz, G.K.H. Madsen, D. Kvasnicka and J. Luitz, *WIEN2K: An Augmented Plane Wave Plus Local Orbitals Program for Calculating Crystal Properties, edited by K. Schwarz*, Vienna University of Technology, Vienna, 2001.

[9] J.P. Perdew and Y. Wang, *Accurate and simple analytic representation of the electron-gas correlation energy*, Phys. Rev. B 45 (1992) p.13244–13249.

[10] J.P. Perdew, S. Kurth, A. Zupan and P. Blaha, *Accurate Density Functional with Correct Formal Properties: A Step Beyond the Generalized Gradient Approximation*, Phys. Rev. Lett. 82 (1999) p.2544–2547.

[11] D. Koller, F. Tran and P. Blaha, *Merits and limits of the modified Becke-Johnson exchange potential*, Phys. Rev. B 83 (2011) p.195134–195143.

[12] D. Koller, F. Tran and P. Blaha, *Improving the modified Becke-Johnson exchange potential*, Phys. Rev. B 85 (2012) p.155109–155116.

[13] F. Tran and P. Blaha, *Accurate Band Gaps of Semiconductors and Insulators with a Semilocal Exchange-Correlation Potential*, Phys. Rev. Lett. 102 (2009) p.226401–226404.

[14] Z. Wu and R.E. Cohen, *More accurate generalized gradient approximation for solids*, Phys. Rev. B 73 (2006) p.235116–235119.

[15] W. Kohn, *Discontinuity of the exchange-correlation potential from a density-functional viewpoint*, Phys. Rev. B 33 (1986) p.4331–4333.

[16] A.D. Becke and E.R. Johnson, *A simple effective potential for exchange*, J. Chem. Phys. 124 (2006) p.221101–221104.

[17] A.D. Becke and M.R. Roussel, *Exchange holes in inhomogeneous systems: A coordinate-space model*, Phys. Rev. A 39 (1989) p.3761–3767.

[18] R.B. Araujo, J.S. de Almeida and A.F. da Silva, *Electronic properties of III-nitride semiconductors: A first-principles investigation using the Tran-Blaha modified Becke-Johnson potential*, J. Appl. Phys. 114 (2013) p.183702–183707.

[19] D.J. Singh, *Electronic structure calculations with the Tran-Blaha modified Becke-Johnson density functional*, Phys. Rev. B 82 (2010) p.205102–205111.

[20] H. Jiang, *Band gaps from the Tran-Blaha modified Becke-Johnson approach: A systematic investigation*, J. Chem. Phys. 138 (2013) p.134115–134121.

[21] Y.H. Zhao, Y.F. Li and Y. Liu, *Half-metallic p-electron ferromagnetism in alkaline earth doped AlAs: A first-principles calculation*, Appl. Phys. Lett. 100 (2012) p.092407–092409.

[22] H.J. Monkhorst and J.D. Pack, *Special points for Brillouin-zone integrations*, Phys. Rev. B 13 (1976) p.5188–5192.

[23] F.D. Murnaghan, *The Compressibility of Media under Extreme Pressures*, Proc. Natl. Acad. Sci. U.S.A. 50 (1944) p.244–247.

[24] K.H. Hellwege, O. Madelung and Landolt-Bornstein, *Semiconductors: Physics of Group IV Elements and III–V Alloys, New Series, Group III*, Vol. 17, Springer-Verlag, Berlin, (1982).

[25] S. Adachi, *Properties of Group-IV III–V and II–VI Semiconductor*, Wiley, West Sussex, 2005.

[26] G. Giesecke and H. Pfister, *Prazisionsbestimmung der Gitterkonstanten von AIII BV-Verbindung*, Acta Crystallogr. 11 (1958) p.369–371.

[27] S.Q. Wang and H.Q. Ye, *Plane-wave pseudopotential study on mechanical and electronic properties for IV and III-V crystalline phases with zinc-blende structure*, Phys. Rev. B 66 (2002) p.235111–235117.

[28] A. Bentouaf, T. Ouahranı, M. Amerı, R. Mebsout and D. Hachemane, *Theoretical study of structural, electronic, optical and thermodynamic properties of AlP, InP and AlAs compounds*, J. Optoelectron. Adv. Mater. 7 (2013) p.659–666.

[29] V. Cimalla, J. Pezoldt, G. Ecke, R. Kosiba, O. Ambacher, L. Spieb, G. Teichert, H. Lu and W.J. Schaff, *Growth of cubic InN on r-plane sapphire*, Appl. Phys. Lett. 83 (2003) p.3468–3470.

[30] A. Tabata, A.P. Lima, L.K. Teles, L.M.R. Scolfaro, J.R. Leite, V. Lemos, B. Schöttker, T. Frey, D. Schikora and K. Lischka, *Structural properties and Raman modes of zinc blende InN epitaxial layers*, Appl. Phys. Lett. 74 (1999) p.362–364.


Downloaded by [Zapadoceska Univerzita], [A Reshak] at 07:57 03 March 2016

[31] J. Schörmann, D.J. As, K. Lischka, P. Schley, R. Goldhahn, S.F. Li, W. Löffler, M. Hetterich and H. Kalt, *Molecular beam epitaxy of phase pure cubic InN*, Appl. Phys. Lett. 89 (2006) p.261903–261905.

[32] M. Aslan, B.G. Yalcin and M. Ustundag, *Structural and electronic properties of Ga1−xInx As1−yNy quaternary semiconductor alloy on GaAs substrate*, J. Alloys Compd. 519 (2012) p.55–59.

[33] C. Stampfl and C.G. Van de Walle, *Density-functional calculations for III-V nitrides using the local-density approximation and the generalized gradient approximation*, Phys. Rev. B 59 (1998) p.5521–5535.

[34] Landolt-Bornstein, *Numerical Data and Functional Relationships in Science and Technology*, Vol. III, O. Madelung, ed., Springer, Berlin, 1972.

[35] M.L. Cohen, *Calculation of bulk moduli of diamond and zinc-blende solids*, Phys. Rev. B 32 (1985) p.7988–7991.

[36] M.E. Sherwin and T.J. Drummond, *Predicted elastic constants and critical layer thicknesses for cubic phase AIN; GaN, and InN on ţ-SiC*, J. Appl. Phys. 69 (1991) p.8423–8425.

[37] L. Vegard, *Formation of Mixed Crystals by Solid-Phase Contact*, J. Phys. 5 (1921) p.393–395.

[38] S. Adachi, *Band gaps and refractive indices of AlGaAsSb, GaInAsSb, and InPAsSb: Key properties for a variety of the 2–4μm optoelectronic device applications*, J. Appl. Phys. 61 (1987) p.4869–4876.

[39] L.C. de Carvalho, A. Schleifeabd and F. Bechstedt, *Influence of exchange and correlation on structural and electronic properties of AlN, GaN, and InN polytypes*, Phys. Rev. B 84 (2011) p.195105–195127.

[40] R. Ahmed, F. Aleem, S.J. Hashemifar and H. Akbarzadeh, *First-principles study of the structural and electronic properties of III-phosphides*, Phys. B 403 (2008) p.1876–1881.

[41] W.J. Turner, W.E. Reese and G.D. Pettit, *Exciton Absorption and Emission in InP*, Phys. Rev. 136 (1964) p.A1467–A1470.

[42] J. Schörmann, D.J. As, K. Lischka, P. Schley, R. Goldhahn, S.F. Li, W. Löffler, M. Hetterich and H. Kalt, *Molecular beam epitaxy of phase pure cubic InN*, Appl. Phys. Lett. 89 (2006) p.261903–261905.

[43] W. Shan, W. Walukiewicz, J.W. Ager III, E.E. Haller, J.F. Geisz, D.J. Friedman, J.M. Olson and S.R. Kurtz, *Band Anticrossing in GaInNAs Alloys*, Phys. Rev. Lett. 82 (1999) p.1221–1224.

[44] K.M. Yu, W. Walukiewicz, J. Wu, J. Beeman, J.W. Ager III, E.E. Haller, W. Shan, H.P. Xin, C.M. Tu and M.C. Ridgway, *Formation of diluted III–V nitride thin films by N ion implantation*, J. Appl. Phys. 90 (2001) p.2227–2234.

[45] J.E. Bernard and A. Zunger, *Electronic structure of ZnS, ZnSe, ZnTe, and their pseudobinary alloys*, Phys. Rev. B 36 (1987) p.3199–3228.

Downloaded by [Zapadoceska Univerzita], [A Reshak] at 07:57 03 March 2016